ORIGINAL ARTICLE
Iran J Allergy Asthma Immunol
June 2022; 21(3):287-299.
Doi: 10.18502/ijaai.v21i3.9802

Immunosuppressive Effects and Potent Anti-tumor Efficacy of mTOR Inhibitor Everolimus in Breast Tumor-bearing Mice

Davoud Rostamzadeh[1,2], Mohammad Reza Haghshenas[1], Mahdi Samadi[1], Zahra Mojtahedi[1], Zohreh Babaloo[2,3], and Abbas Ghaderi[1]

[1] Shiraz Institute for Cancer Research, School of Medicine, Shiraz University of Medical Sciences, Shiraz, Iran
[2] Department of Immunology, School of Medicine, Tabriz University of Medical Sciences, Tabriz, Iran
[3] Immunology Unit, Drug Applied Research Center, Tabriz University of Medical Sciences, Tabriz, Iran

Received: 18 May 2021; Received in revised form: 21 February 2022; Accepted: 27 February 2022

ABSTRACT

To investigate the effects of everolimus, a mechanistic/mammalian target of rapamycin (mTOR) inhibitor, on tumor growth and immune response in a mouse model of breast cancer.

Human hormone receptor-positive (HR+)/human epidermal growth receptor 2-negative (HER2-) MC4-L2 cell line was used to establish a mouse model of breast cancer. The inhibitory effects of high (10 mg/kg) and low (5 mg/kg) doses of everolimus were investigated on tumor growth. Additionally, the frequency of $CD4^+Foxp3^+$ regulatory T cells (Tregs), $CD8^+Foxp3^+$ Tregs, and $CD4^+$ and $CD8^+$ T cells expressing cytotoxic T-lymphocyte-associated antigen-4 (CTLA-4) was explored by flow cytometry in bone marrow, lymph nodes, and spleen.

Our results showed that both 10 mg/kg and 5 mg/kg doses of everolimus efficiently inhibited tumor growth, resulting in reduced breast tumor volume. In addition, it was revealed that everolimus-treated mice induced a higher frequency of $CD4^+Foxp3^+$ Tregs, $CD8^+Foxp3^+$ Tregs, and $CD4^+Foxp3^+CTLA\text{-}4^+$ Tregs as well as $CD4^+$ and $CD8^+$ T cells expressing CTLA-4 in their bone marrow, lymph nodes, and spleen compared with standard control (vehicle-treated) in a dose-dependent manner. Furthermore, we found that everolimus treatment with 10 mg/kg and 5 mg/kg increased the frequency of $Helios^+Foxp3^+$ Tregs in the bone marrow of treated mice compared with the control group.

Our results indicate that treatment with everolimus not only inhibits tumor growth but also exerts an immunomodulatory effect by inducing Tregs in the lymphoid organs of breast cancer-bearing mice. The combination of therapy with other anti-cancer agents may negate immune suppression and improve the efficacy of mTOR-targeted breast cancer therapy.

Keywords: CTLA-4 antigen; Everolimus; Regulatory T-lymphocytes

Corresponding Authors: Abbas Ghaderi, PhD;
Shiraz Institute for Cancer Research, Department of Immunology, School of Medicine, Shiraz University of Medical Science, Shiraz, Iran. Tel: (+98 71) 3235 1452, Fax: (+98 71) 3230 4952, E-mail: ghaderia@sums.ac.ir, ghaderia@gmail.com

Zohreh Babaloo, PhD;
Department of Immunology, School of Medicine, Tabriz University of Medical Sciences, Tabriz, Iran. Postal Code: 5166614766 Tel/Fax: (+98 41) 3336 4665, E-mail: Zbabaloo20@gmail.com, Zbabaloo@tbzmed.ac.ir

Copyright © 2022 Rostamzadeh et al. Published by Tehran University of Medical Sciences.

This work is licensed under a Creative Commons Attribution-NonCommercial 4.0 International license (https://creativecommons.org/licenses/by-nc/4.0/). Non-commercial uses of the work are permitted, provided the original work is properly cited.

INTRODUCTION

The mechanistic/mammalian target of rapamycin (mTOR) adaptor, an important downstream target of phosphatidylinositol-3-kinase (PI3K)/AKT, is an evolutionarily conserved serine/threonine-protein kinase. It belongs to the Phosphatidylinositol-3 kinase-related kinases (PIKK) family and plays significant roles in cell growth, metabolism, protein synthesis, proliferation, survival, apoptosis, and autophagy.[1] In cancer, oncogenic activation of the PI3K/AKT/mTOR signaling pathway was associated with several processes required for the cancer initiation, progression, metastasis, and resistance to therapy.[2] The PI3K/AKT/mTOR pathway regulation is frequently disrupted in various cancer types, including breast cancer, colorectal cancer, pancreatic cancer, and hematologic malignancies, which highlights the value of targeting this pathway as an attractive and promising therapeutic approach against cancer.[3,4] Thus, mTOR inhibition has attracted significant attention in cancer therapy, and mTOR inhibitors such as rapamycin and everolimus have exhibited potent antitumor activity against a wide variety of solid tumors, both *in vitro* and *in vivo*.[5-7] Consequently, the FDA has approved the use of mTOR inhibitor everolimus in the treatment of various malignancies, including advanced recurrent human hormone receptor-positive (HR+)/human epidermal growth receptor 2-negative (HER2-) breast cancer.[8]

mTOR signaling pathway has emerged as a critical regulator in immune and inflammatory responses and metabolic reprogramming to maintain the proper immune function.[9,10] In T lymphocytes, mTOR activity, appears to direct the differentiation of $CD4^+$ T cells into T helper (Th) 1, Th2, Th17, and regulatory T cells (Tregs). Ras homolog enriched in the brain (Rheb) /mTORC1 deficient T cells fail to polarize into Th1 and Th17 subsets *in vitro* and *in vivo* and lose their ability to develop the classical experimental autoimmune encephalomyelitis (EAE). Moreover, deletion or knockdown of the mTORC2 component raptor-independent companion of TOR (Rictor), an essential subunit of mTORC2 in T cells, inhibits their capacity to become Th2 but preserves their ability to shift toward Th1 and Th17 subgroups.[11,12] Rapamycin, as an mTOR inhibitor, facilitates the generation of forkhead box P3 (Foxp3) + Treg cells without transforming growth factor-beta (TGF-β).[13] mTOR inhibitor-based immunosuppression treatment regimen for solid transplantation selectively enhanced $CD4^+CD25^+Foxp3^+$ Tregs and improved the immunosuppressive environment required for preventing graft rejection.[14,15] These reports suggest that everolimus treatment could potentially affect the outcome of the immune system, which, in turn, may affect the clinical results of patients with cancer treated with mTOR inhibitors. However, in contrast to rapamycin, little is known about the immunological effects of everolimus treatment. In such terms, this study aimed to explore the impact of everolimus on tumor growth and immune status in the lymph nodes, spleen, and bone marrow of $HER2^-/ER^+$ breast tumor-bearing mice.

MATERIALS AND METHODS

Ethics Statement

The Ethics Committee at Shiraz University of Medical Sciences (IR.SUMS.MED.REC.1397.444) and Tabriz University of Medical Sciences (Grant/Award Number: 96/51) approved the experiments. All the surgery and euthanasia were performed under injections of intraperitoneal ketamine (100 mg/kg IP) and xylazine (10 mg/kg IP). All efforts were made to minimize the number of animals used and reduce animal suffering.

Cell Line and Culture

The BALB/c-derived mouse mammary adenocarcinoma $HER2^-/ER^+$ cell line MC4-L2 was purchased from the Iranian Biological Resource Center (IBRC) (Tehran, Iran). Cells were maintained in a T75 flask in Dulbecco's Modification of Eagle's Medium (DMEM)/Ham's F12 (Gibco/Invitrogen, Carlsbad, CA, USA) medium. Cell media was supplemented with 2 mM of L-Glutamine, 15 mM of HEPES buffer growth medium, 10% of heat-inactivated fetal bovine serum (FBS, Gibco BRL, Life Technologies, Grand Island, NY), and 100 IU/mL of penicillin and 100 mg/mL of streptomycin (Gibco/Invitrogen). The cell-containing flask was incubated at 37°C in a humidified atmosphere with 5% CO2. Once the cells reached a confluence of approximately 80–90%, the MC4-L2 cells were dislodged from the flask and then washed twice for 5 minutes in phosphate-buffered saline (PBS).

Experimental Animals and Tumor Model

Female BALB/c, 5 to 6 weeks of age (body weight range of 20–22 g), were provided from the Pasteur Institute of Iran, Tehran, Iran. Animals were

maintained in an animal care facility in the Medical Physics Research Center of Shiraz University of Medical Sciences under controlled conditions.[16,17] The animals were allowed to adapt to their food and environment for at least one week before starting the experiment. MC4-L2 cells were subcutaneously inoculated at a concentration of 3×10^6 cells in 100 µg sterile 1x PBS into the mammary fat pad of the BALB/c mice and allowed to grow. MC4-L2 cells were injected at viability of greater than 98%. Tumor growth was monitored every 2 to 3 days and approximately 10–14 days following the inoculation of the HER2-/ER+ MC4-L2 cells; the tumors were palpable in the injected areas.

Drug Preparation and Experimental Design

When the tumors reached approximately 100 mm^3 in volume, the tumor-bearing mice were randomly assigned into three groups of five animals to receive either everolimus or vehicle. Everolimus was purchased from Medscheme Express (Monmouth Junction, NJ, USA) and was dissolved in 0.5% carboxymethyl cellulose sodium salt (CMC; Wako Pure Chemical Industries, Ltd., Osaka, Japan) just before its administration to the mice. Treatment groups consisted of: (1) Group A received the highest everolimus dose of 10 mg/kg everolimus per day, (2) group B received 5 mg/kg everolimus per day, and (3) group C served as the control group (vehicle-treated animals' group), and received vehicle (0.5% CMC). Everolimus and vehicle were orally administered five times a week only via gavage in a volume of 100 µL. Mice received either everolimus or an equivalent volume of vehicle for three weeks.

Tumor Volume, Body Weight, and Weight Measurement

All groups' tumor volumes and body weights were monitored on the first day of everolimus administration. Tumor volumes were measured and recorded every three days using a digital caliper. They were calculated using the formula $V = (L \times 2)/2$, where tumor length (L) is the largest diameter of the tumor and width (W) is the shortest diameter. As well, the body weights of mice were recorded every three days. After three weeks of treatment, the mice were euthanized, the tumor tissues were harvested, and tumor weights were measured and recorded immediately after being collected from the mice.

Preparation of Mononuclear Cell Suspension from Bone Marrow, Spleen, and Lymph Nosed

As previously described, the single-cell suspension was mechanically prepared from the bone marrow, spleen, and lymph nodes.[16,17,18] Cell viability was found to be greater than 98%, and all the preparation procedures were done at 4°C.

Antibodies and Flow Cytometry Analysis

PerCP/Cy5.5-conjugated anti-mouse CD4 (Clone PM4-4), Alexa Fluor-488-conjugated anti-mouse CD8 (Clone 53-6.7), phycoerythrin (PE)-conjugated anti-mouse CD3 (Clone 17A2), and allophycocyanin (APC)-conjugated anti-mouse PD-1 (Clone PMP1-30) were used for cell-surface marker detection. After fixation and permeabilization, the cells were intracellularly stained with PE-conjugated anti-mouse/rat/human Foxp3 (Clone 150D), APC-conjugated anti-mouse CTLA-4 (Clone UC10-4B9), and APC-conjugated anti-mouse/human Helios (a marker of thymic derived regulatory T cells) (clone 22F6) antibodies. All the antibodies were obtained from Biolegend Inc (San Diego, CA, USA). FACSCalibur flow cytometer (BD Bioscience, San Jose, CA) was used to determine the frequency of stained cells. Matched fluorescently-labeled isotype and fluorescence minus one (FMO) controls were also employed to determine the probable background levels of staining and ensure immunostaining specificity.

Statistical Analysis

Statistical analyses were performed using GraphPad Prism version 6.0 (GraphPad Software, Inc., San Diego, USA). Flow cytometry data were analyzed with FlowJo v10.0.6 software (Tree Star, Ashland, OR). All the groups were tested for normality with the Shapiro–Wilk method. Kruskal–Wallis test followed by Dunn's post hoc multiple comparison test was utilized for statistical analysis. Data were presented as mean±Standard Error of Mean (SEM). In all comparisons, $p<0.05$ was considered statistically significant.

RESULTS

***In Vivo* Activity of Everolimus in Tumor-bearing Mice**

We first evaluated the administration of the mTOR inhibitor everolimus on tumor growth in mice bearing

MC4-L2 breast tumors. Once the tumor volume reached approximately 100 mm^3 (day 1), mice were randomly divided into three groups (n=5). Mice then received vehicle only (vehicle-treated animals), a high dose (10 mg/kg), and a low dose (5 mg/kg) of everolimus orally five times per week for three weeks. Administration of everolimus (5 mg/kg and 10 mg/kg) to tumor-bearing mice during treatment produced no apparent morbidity and/or mortality. We observed that treatment with everolimus efficiently arrested breast tumor growth or showed a tendency towards decreased throughout treatment. Interestingly, everolimus showed dose-dependent antitumor activity, and our results demonstrated that 10 mg/kg everolimus was more efficient and significantly suppressed tumor growth after 14 days of treatment (p=0.002). The suppressive effect of everolimus on tumor growth in the 5 mg/kg (p=0.002) and 10 mg/kg (p=0.001) everolimus-treated groups on day 21 was statistically significant compared with the vehicle-treated control animals. Meanwhile, in the vehicle-treated group, the tumor size increased throughout treatment. Tumor-volume ratios at the end of the study were 462.5±85.1 mm^3 for the vehicle-treated control animals; 178.4±32.5 mm^3 for mice treated with everolimus at 5 mg/kg; and 125.6±25.2 mm^3 for the 10 mg/kg everolimus treated group. The tumor volume from the beginning to the end of treatment is shown in Figure 1A. We determined the tumor weight at the end of the experiment to further explore the effects of everolimus on tumor growth. Tumor weights were significantly reduced in the groups treated with 10 mg/kg (310±40 mg, p=0.03) and 5 mg/kg (318±33 mg, p=0.01) everolimus as compared with the vehicle-treated animals (824±120 mg). Harvested tumors were weighed at the end of the treatment period, as shown in Figures 1B and C. The tumor weights significantly decreased by 38.5 and 38.1% after being treated with low (5 mg/kg) and high (10 mg/kg) dosages of everolimus compared with the vehicle-treated animals, respectively. During the treatment, weight loss was observed in the high (10 mg/kg) and low (5 mg/kg) dosage everolimus-treated groups. Whereas the vehicle-treated mice continued to gain weight throughout the treatment, the everolimus-treated groups started weight loos on the approximately 8th day after the introduction of the mTOR inhibitor and continued throughout treatment. Final body weight curves indicated that the everolimus-treated mice had significant reductions in both the 10 mg/kg (14.4±0.24 gr, p=0.03) and 5 mg/kg (15.62±0.24 gr, p=0.01) treated groups as compared to the vehicle-treated control group (22±0.31 gr) **(**Figure 1D). Thus, in addition to the inhibitory effect of everolimus on tumor growth, everolimus was capable of promoting weight loss and might worsen the clinical status of the animals.

Everolimus Treatment Results in an Increase in the Frequency of $CD4^+$ $Foxp3^+$ Treg Cells and $CD4^+$ $CTLA\text{-}4^+$ T Cells in the Bone Marrow of Tumor-bearing Mice

We initially measured the percentages of Foxp3- and cytotoxic T-lymphocyte-associated antigen-4 (CTLA-4) -expressing $CD4^+$ and $CD8^+$ T cells in freshly isolated bone marrow mononuclear cells (BMNCs) of tumor-bearing mice. A representative gating strategy for immunophenotyping of these populations by flow cytometry is shown in Figure 2 A. In the bone marrow, there was no significant difference in the mean frequencies of $CD4^+$ and $CD8^+$ T cells and the mean $CD4^+/CD8^+$ ratio between both 5 mg/kg and 10 mg/kg everolimus-treated groups and the vehicle group (data not shown). In addition, we observed higher frequencies of $CD4^+Foxp3^+$ Treg cells and $CD4^+CTLA\text{-}4^+$ T cells in the mice from both the 5 mg/kg and 10 mg/kg everolimus-treated groups in comparison with the vehicle-treated mice in the bone marrow. However, the frequency of $CD4^+Foxp3^+$ Treg cells (p=0.01) and $CD4^+CTLA\text{-}4^+$ T cells (p=0.03) in the bone marrow of 10 mg/kg everolimus-treated mice were significantly higher than that of the vehicle control group mice (Table 1). This increase was dose-dependent, as the frequency of $CD4^+Foxp3^+$ Treg cells and $CD4^+CTLA\text{-}4^+$ T cells were higher in the 10 mg/kg treated group than in the 5 mg/kg treated group (Figure 2B). We then evaluated the frequency of the total $CD8^+Foxp3^+$ Tregs and $CD8^+CTLA\text{-}4^+$ cells. Despite the significantly lower level of Foxp3 and CTLA-4 expressing $CD8^+$ T cells, everolimus-treated groups exhibited a slightly dose-dependent increase in frequency (Figure 2B) (Table 1). The geometric mean fluorescence intensity (gMFI) for Foxp3 and CTLA-4 in the $CD4^+Foxp3^+$ Treg cells and $CD4^+CTLA\text{-}4^+$ T cell populations showed an increase in a dose-dependent manner in everolimus-treated mice groups (Figure 2C).

Table 1. The frequency of $CD4^+$ and $CD8^+$ expressing Foxp3 and CTLA-4 in the bone marrow of 5 mg/kg and 10 mg/kg everolimus-treated groups and vehicle groups.

Subpopulation	$CD4^+$ $Foxp3^+$ Treg cells (Mean ±SEM)	$CD4^+$ $CTLA\text{-}4^+$ T cells (Mean ±SEM)	$CD8^+$ $Foxp3^+$ Treg cells (Mean ±SEM)	$CD8^+$ $CTLA\text{-}4^+$ T cells (Mean ±SEM)
Vehicle (n=5)	12.1±1.83	24.3±4.47	0.32±0.05	0.64±0.07
5 mg/kg EVL (n=5)	15.2±2.73	28.1 ± 5.0	0.42 ± 0.03	0.77±0.06
p-value	0.17	0.07	>0.99	>0.99
10 mg/kg EVL (n=5)	20.3±4.33	32.2±5.80	0.47±0.05	0.86±0.08
p-value	**0.01**	**0.03**	0.35	0.26

SEM, standard error of the mean; ns, not significant; EVL, everolimus

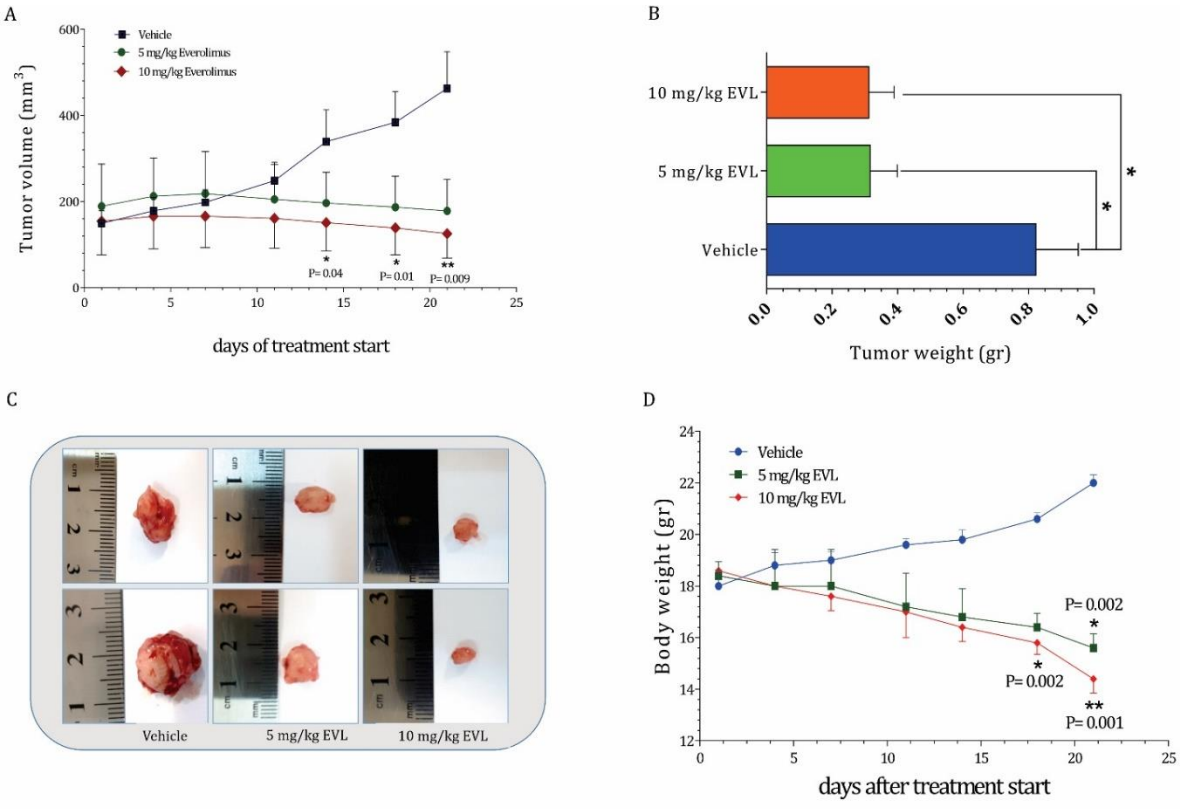

Figure 1. Everolimus treatment showed potent antitumor activity against MC4-L2 tumor-bearing mice

Inbreed BALB/c mice were inoculated with mouse mammary adenocarcinoma cell line MC4-L2. When the average size of tumors reached approximately 100 mm^3, the tumor-bearing were treated with vehicle or 10 mg/kg and 5 mg/kg per day everolimus five times per group for three weeks. Tumor volume and animal weights were measured every 3 days as described above. (A) The graph shows tumor size with time after everolimus or vehicle treatment in breast cancer-bearing mice. (B) Both 10 mg/kg and 5 mg/kg everolimus treatment markedly reduced the tumor weight at the end of the experiment. (C) Freshly isolated tumors from mice-bearing breast tumors represented potent growth inhibitory effects of everolimus *in vivo*. (D) Contrary to the vehicle-treated group, body-weight curves indicated that everolimus-treated mice showed a significant reduction in weight gain from the last 3 days of the treatment period. Data are presented as mean tumor volume±standard error of the mean (SEM); * $p<0.05$; ** $p<0.01$; *** $p<0.001$, Kruskal–Wallis test followed by Dunn's post hoc multiple comparisons. N=5 mice/group.

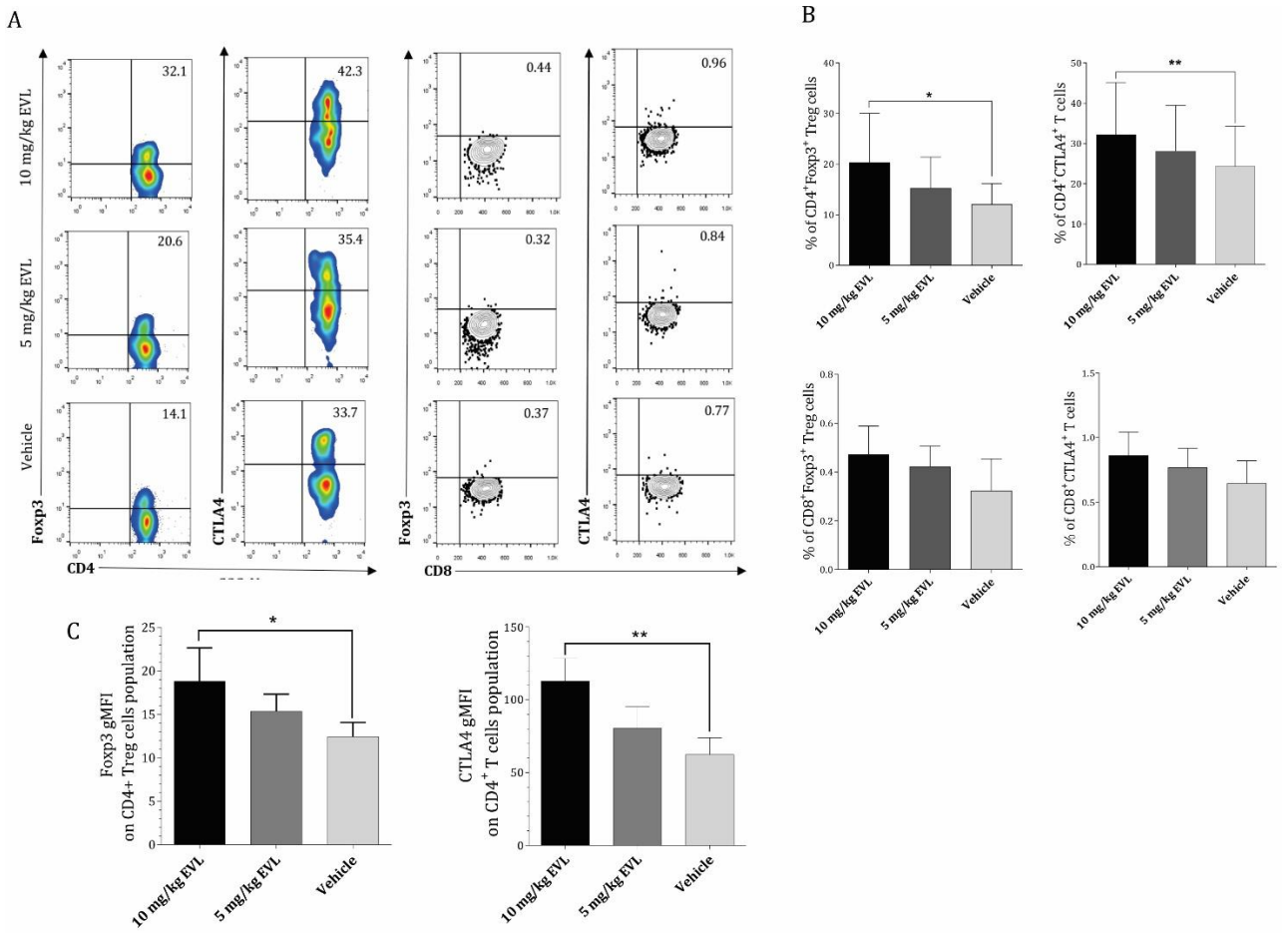

Figure 2. Flow cytometry analysis of CD4$^+$Foxp3$^+$ Treg cells and CD4$^+$CTLA-4$^+$ T cells in bone marrow mononuclear cells from breast cancer of mice treated with 10 mg/kg and 5 mg/kg everolimus. Immediately after all the mice were killed, uniform single-cell suspensions from each group were prepared from freshly removed lymph nodes, bone marrow, and spleens. The cells were incubated and stained with specific fluorochrome-conjugated antibodies, and finally, the cells were resuspended in 500 µL of flow cytometry–staining solution and analyzed using FACSCalibur flow cytometer. (A) Representative flow cytometry analysis of CD4$^+$Foxp3$^+$ Treg cells and CD4$^+$CTLA-4$^+$ T cell population from freshly isolated mononuclear cells from the bone marrow of 5 mg/kg and 10 mg/kg everolimus-treated groups and vehicle group. (B) Representative graphs of CD4$^+$Foxp3$^+$ Tregs, CD8$^+$Foxp3$^+$ Tregs, and CD4$^+$ and CD8$^+$ T cells expressing CTLA-4 from the bone marrow of 5 mg/kg and 10 mg/kg everolimus-treated groups and vehicle group. (C) Representative graph showing the geometric mean fluorescence intensity (gMFI)±SEM of Foxp3 and CTLA-4 in CD4$^+$ T cells isolated from the bone marrow of 5 mg/kg and 10 mg/kg everolimus-treated groups and vehicle group.

*** p<0.05; ** p<0.01; *** p<0.001, Kruskal–Wallis test followed by Dunn's post hoc multiple comparisons. N=5 mice/group.**

Everolimus Treatment Increases the Frequency of CD4$^+$Foxp3$^+$ Treg Cells and CD4$^+$CTLA-4$^+$ T Cells in the Spleen and Lymph Nodes of Breast Tumor-bearing Mice

Then, we studied the frequency of CD4$^+$Foxp3$^+$Treg cells and CD4$^+$CTLA-4$^+$ T cells from the lymph nodes and spleen of everolimus-treated mice. As shown in Figure 3, both lymph nodes and spleen from 10 mg/kg and 5 mg/kg everolimus-treated mice showed a higher frequency of CD4$^+$Foxp3$^+$ Tregs, CD8$^+$Foxp3$^+$ Tregs, and CD4$^+$ and CD8$^+$ T cells expressing CTLA-4 compared to the vehicle group (Table 2 and 3). Our results showed that the effects of everolimus on the Foxp3-and CTLA-4-expressing

$CD4^+$ and $CD8^+$ T cells were dose-dependent, and 10 mg/kg administration of everolimus increased immunosuppressive molecules in both the spleen and lymph nodes more efficiently (Figure 3 B-I). The gMFI Foxp3 and CTLA-4 expression by $CD4^+$ and $CD8^+$ T cells from spleen and lymph nodes were higher than in the control group. However, this result is not statistically significant (Figure 3 J-M). In addition, everolimus-treated mice showed increased $CD4^+Foxp3^+CTLA\text{-}4^+$ Treg in bone marrow, lymph nodes, and spleen. For note, in contrast to lymph nodes, the effects of everolimus on $CD4^+Foxp3^+CTLA\text{-}4^+$ Treg cells frequency were dose-dependent, and the results of 10 mg/kg of everolimus in the bone marrow and spleen were statistically significant (bone marrow; p=0.01, spleen; p=0.01, lymph nodes; p=0.07) (Figure 4A and B). Together, these findings suggest that everolimus treatment increases the frequency of Treg cells, probably resulting in immunosuppression and tumor progression.

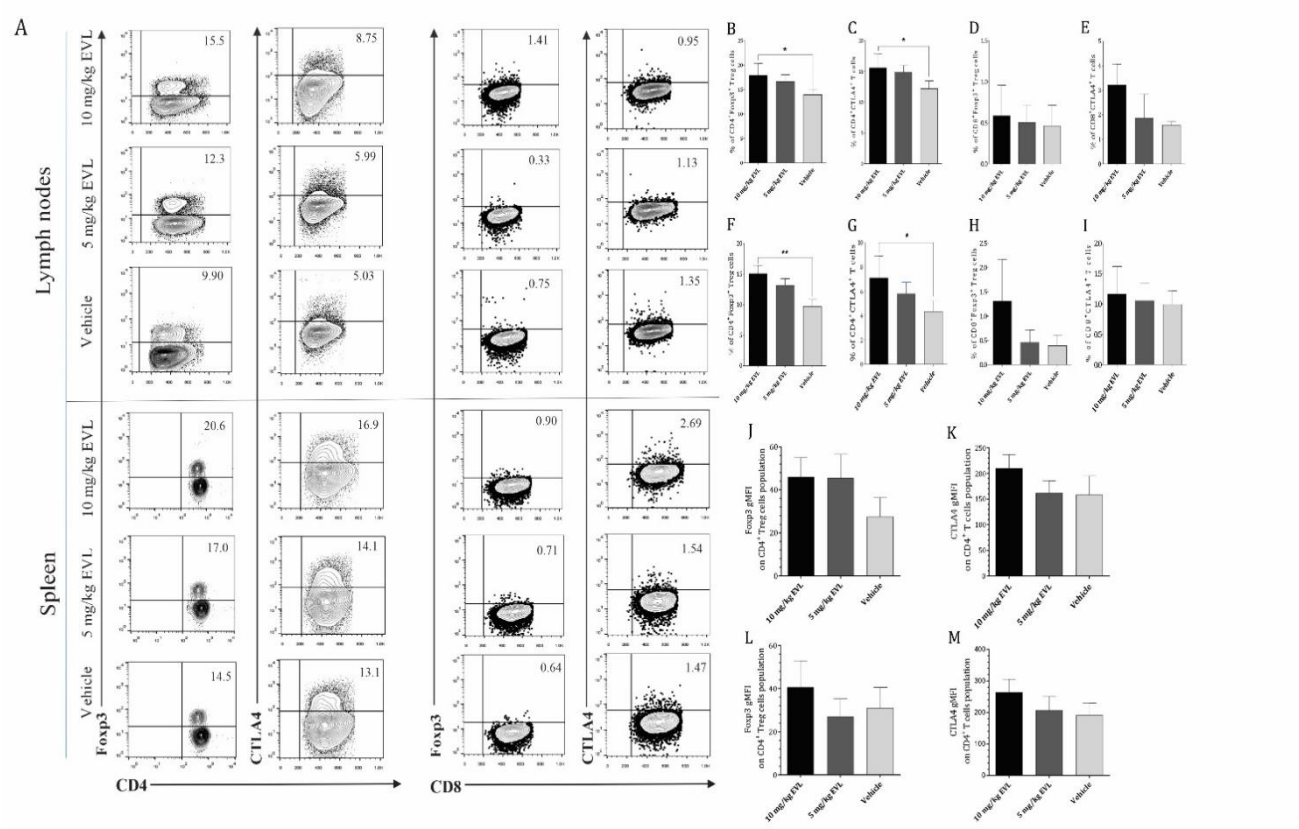

Figure 3. Flow cytometry analysis of $CD4^+Foxp3^+$ Treg cells and $CD4^+CTLA\text{-}4^+$ T cells in the lymph nodes and spleen of mice treated with 10 mg/kg and 5 mg/kg everolimus A) Representative flow cytometry analysis of $CD4^+Foxp3^+$ Treg cells and $CD4^+CTLA\text{-}4^+$ T cell population from freshly isolated mononuclear cells from spleen (lower panels) and lymph nodes (upper panels) of 5 mg/kg and 10 mg/kg everolimus-treated groups and vehicle group. (B, C, D, and E) Representative graphs of $CD4^+Foxp3^+$ Treg cells and $CD4^+CTLA\text{-}4^+$ T cells in the spleen of 5 mg/kg and 10 mg/kg everolimus-treated groups and vehicle group. (F, G, H, and I) Representative plots of $CD4^+$ $Foxp3^+$ Treg cells and $CD4^+$ $CTLA\text{-}4^+$ T cells in lymph nodes of mice treated 5 mg/kg and 10 mg/kg everolimus-treated groups and vehicle group. (J, K, L, and M) The expression of Foxp3 and CTLA-4 on the $CD4^+$ T cell population was shown as the gMFI for each tissue which showed that everolimus enhanced Foxp3 and CTLA4 expression in spleen and lymph nodes after administration of everolimus.

*** p<0.05; ** p<0.01; *** p<0.001, Kruskal–Wallis test followed by Dunn's post hoc multiple comparisons. N=5 mice/group.**

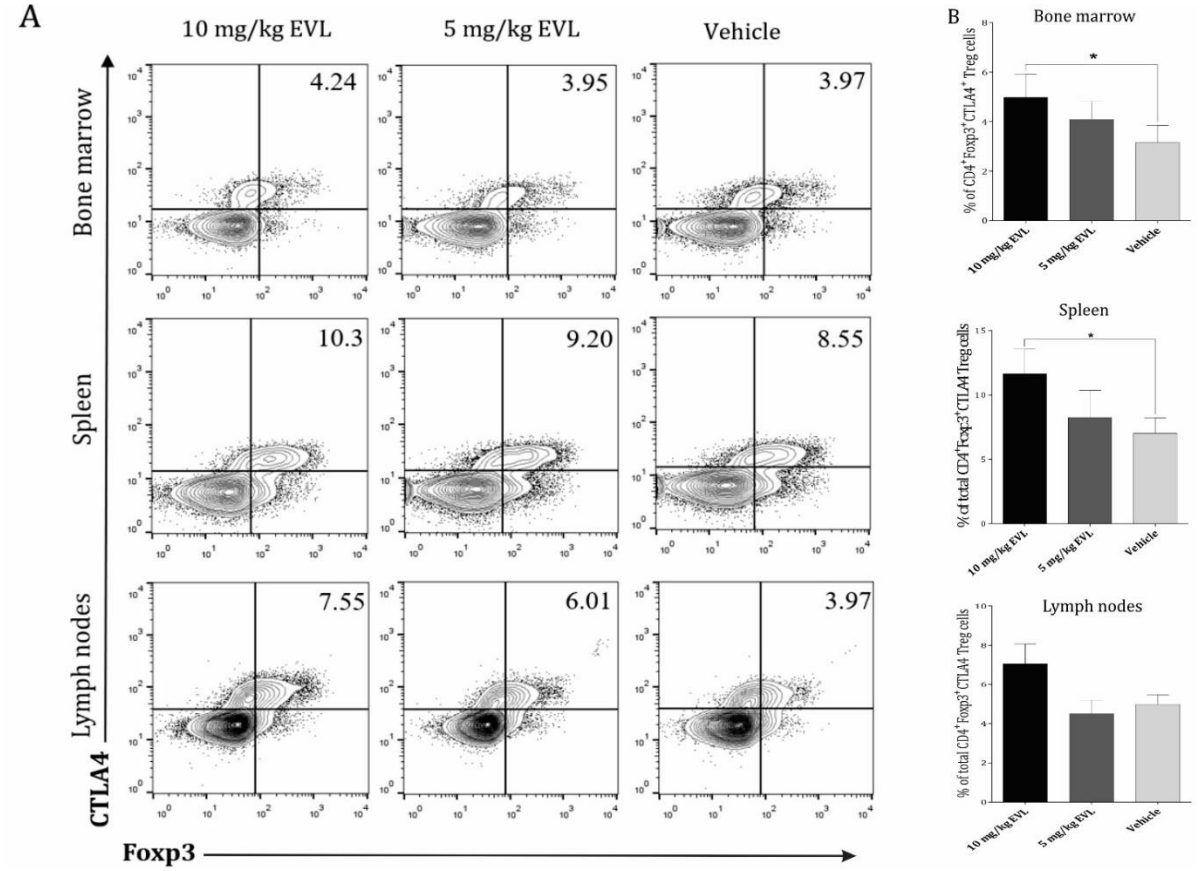

Figure 4. Effect of everolimus treatment on CD4$^+$Foxp3$^+$CTLA-4$^+$ Treg cells in the lymph nodes of mice-treated with 10 mg/kg and 5 mg/kg everolimus (A) Phenotyping analysis of CD4$^+$Foxp3$^+$CTLA-4$^+$ Treg cells in lymph nodes, spleen, and bone marrow, from 5 mg/kg and 10 mg/kg everolimus groups and vehicle group. (B) Graphs represent the mean frequencies of CD4$^+$Foxp3$^+$CTLA-4$^+$ Treg cells in bone marrow, lymph nodes, and spleen from 5 mg/kg and 10 mg/kg everolimus-treated and vehicle groups.

*** p<0.05; ** p<0.01; *** p<0.001, Kruskal–Wallis test followed by Dunn's post hoc multiple comparisons. N=5 mice/group.**

Table 2. The frequency of CD4$^+$ and CD8$^+$ expressing Foxp3 and CTLA-4 in the spleen of 5 mg/kg and 10 mg/kg everolimus-treated groups and vehicle group

Subpopulation	CD4$^+$ Foxp3$^+$ Treg cells (Mean ± SEM)	CD4$^+$ CTLA-4$^+$ T cells (Mean ± SEM)	CD8$^+$ Foxp3$^+$ Treg cells (Mean ± SEM)	CD8$^+$ CTLA-4$^+$ T cells (Mean ± SEM)
Vehicle (n= 5)	13.9±0.51	12.2±0.56	9.7±0.54	4.3±0.41
5 mg/kg EVL (n=5)	16.6±0.61	14.8±0.49	13.1 ± 0.48	5.8±0.42
p-value	0.11	0.12	>0.99	>0.99
10 mg/kg EVL (n=5)	17.9±1.07	15.5±1.03	15.1 ± 0.61	7.09±0.8
p-value	**0.02**	**0.02**	>0.99	0.06

SEM, standard error of the mean; ns, not significant; EVL, everolimus

Table 3. The frequency of $CD4^+$ and $CD8^+$ expressing Foxp3 and CTLA-4 in the lymph nodes of 5 mg/kg and 10 mg/kg everolimus-treated groups and vehicle group

Subpopulation	$CD4^+$ $Foxp3^+$ Treg cells (Mean±SEM)	$CD4^+$ $CTLA\text{-}4^+$ T cells (Mean ± SEM)	$CD8^+$ $Foxp3^+$ Treg cells (Mean±SEM)	$CD8^+$ $CTLA\text{-}4^+$ T cells (Mean±SEM)
Vehicle (n=5)	0.46±0.11	1.58±0.09	0.39±0.09	0.99±0.1
5 mg/kg EVL (n=5)	0.5±0.09	1.86±0.43	0.46±0.11	1.06±0.13
p-value	0.12	0.26	>0.99	>0.99
10 mg/kg EVL (n=5)	0.58±0.16	3.21±0.38	1.3±0.38	1.16±0.21
p-value	**0.003**	**0.03**	0.06	>0.99

SEM, standard error of the mean; ns, not significant; EVL, everolimus

Everolimus Treatment Showed Higher Frequencies of the Total Helios-expressing $CD4^+$ and $CD8^+$ T Cells in Bone Marrow

We also evaluated the expression of Helios, a Treg-associated marker, on the $CD4^+$ and $CD8^+$ T cell populations in the bone marrow. Compared to the vehicle group, both 5 mg/kg and 10 mg/kg everolimus-treated mice showed a higher percentage of $CD4^+Helios^+$ and $CD8^+Helios^+$ T cells in their bone marrow. We observed a significant increase in Helios expression on the $CD4^+$ compartment in the mice treated with 10 mg/kg everolimus (p=0.007) compared to the vehicle-treated group (Table 4). Although the expression of Helios on the $CD8^+$ T cell population in everolimus-treated mice was higher than that of the vehicle group, no significant differences in Helios expression between the groups were observed. (Figure 5A, B, and C). Of note, the expression of Helios by $CD4^+$ and $CD8^+$ T cells was observed to be dose-dependent. Similar patterns were observed when Helios expression was analyzed with MFI in the $CD4^+$ and $CD8^+$ T cell populations. We also examined the frequency of bone marrow $CD4^+Foxp3^+Helios^+$ T cells, and the results indicated that everolimus therapy leads to a dose-dependent increase in $CD4^+Foxp3^+Helios^+$ Treg cell numbers (Figure 5D and E). Notably, when the bone marrow cells were gated on $CD4^+Foxp3^+$ T cells and analyzed for Helios expression, Helios was expressed on 33.1%, 31.3%, and 20.9% of $CD4^+Foxp3^+$ Treg cells in 10 mg/kg, 5 mg/kg, and vehicle-treated mice, respectively (Figure 5F). Together, these findings indicate that everolimus induces the expansion of Helios-expressing Tregs in the bone marrow of breast cancer-bearing mice.

Table 4. The frequency of $CD4^+$ and $CD8^+$ expressing Helios in the bone marrow of 5 mg/kg and 10 mg/kg everolimus-treated groups and vehicle group

Subpopulation	$CD4^+$ $Helios^+$ T cells (Mean ± SEM)	$CD8^+$ $Helios^+$ T cells (Mean ± SEM)	$CD4^+$ $Foxp3^+$ $Helios^+$ Treg cells (Mean ± SEM)
Vehicle (n=5)	29.3±1.92	4.59±0.41	7.92±0.7
5 mg/kg EVL (n=5)	33.8±0.7	5.55±1.09	12.8±0.8
p-value	0.47	>0.99	0.23
10 mg/kg EVL (n=5)	37.5±1.41	7.98±1.21	17.9±1.1
p-value	**0.007**	0.18	**0.001**

SEM, standard error of the mean; ns, not significant; EVL, everolimus

Published by Tehran University of Medical Sciences (http://ijaai.tums.ac.ir)

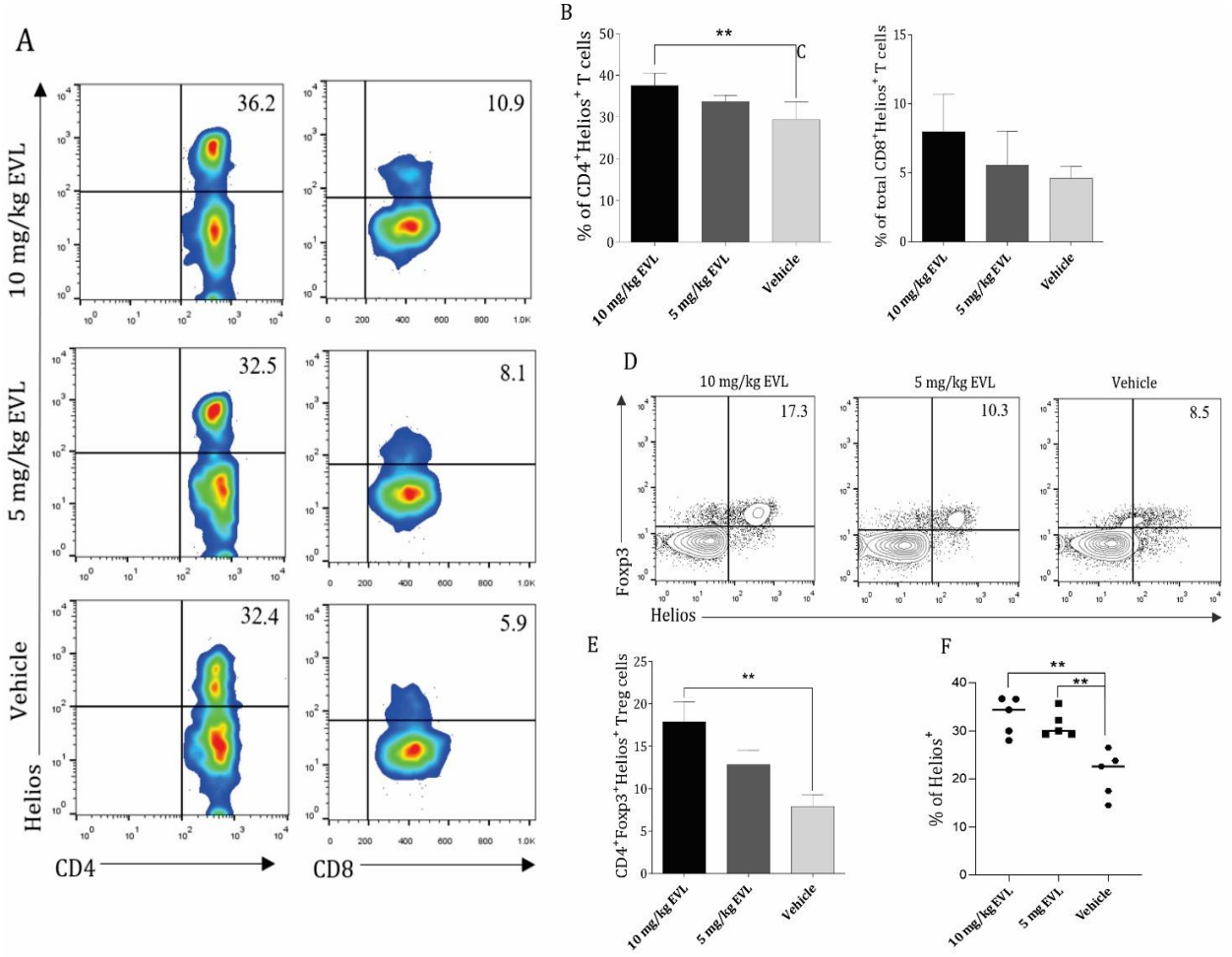

Figure 5. The administration of everolimus on the expression of Helios on CD4$^+$ and -CD8$^+$ T cells in the bone marrow of mice treated with 10 mg and 5 mg everolimus A) Representative flow cytometric analysis of Helios expression on bone marrow CD4$^+$ and -CD8$^+$ T cells. (B and C) Representative graphs of CD4$^+$ and -CD8$^+$ T cells expressing Helios in the bone marrow of mice treated with 10 mg and 5 mg everolimus. (D and E) Representative flow cytometry analysis of CD4$^+$ Foxp3$^+$ Helios$^+$ Treg cells in the bone marrow of mice treated with 10 mg and 5 mg everolimus. (F) The usual graph indicates the percentage of Helios+ cells in the CD4+Foxp3+ Treg cells population.

*** p<0.05; ** p<0.01; *** p<0.001, Kruskal–Wallis test followed by Dunn's post hoc multiple comparisons. N=5 mice/group.**

DISCUSSION

In our study, everolimus at 10 mg/kg and 5 mg/kg doses exhibited a potential inhibitory effect on HER2$^-$/ER$^+$ breast tumors. They reduced the tumor size and volume in MC4-L2-bearing mice dose-dependently. Additionally, the evaluation of wet tumor weights demonstrated a similar pattern between the 10 mg/kg and 5 mg/kg treated groups. The everolimus-treated groups showed a significantly reduced tumor weight compared to the vehicle-treated animal group. We also found that everolimus treatment decreased body weight loss in mice.

Either alone or combined with other anticancer agents or immunotherapy based on blockade of immune checkpoint molecules, everolimus has shown potential growth inhibitory and anti-metastatic activities against different tumor types.[19-21] Several cancer studies have demonstrated that everolimus treatment significantly impairs cell proliferation in a dose- and time-dependent manner. These effects are mediated by modulating 4E-BP1 and S6K1 activity, two major downstream effectors of mTORC1.[7,22-24].

Everolimus treatment over 2 and 4 weeks was sufficient to markedly suppress tumor growth and reduce tumor weight in mice bearing MDA-MB-231-

derived tumors.[20] The inhibitory effect of everolimus was reported to be through the induction of apoptosis by stopping B cell lymphoma (Bcl)-2 and Bcl-w and upregulating the expression levels of caspase-3 and caspase-8 in breast cancer cells. *In vivo* assays showed the potent anti-tumor efficacy of everolimus treatment in the mice bearing MCF-7 tumors.[6] However, the exact mechanism by which everolimus suppresses the growth and tumorigenesis of breast cancer cells remains to be fully elucidated. Still, everolimus treatment has been associated with autophagy and reduces ER expression in aromatase inhibitor-resistant breast cancer.[25] The results of this study demonstrated that everolimus inhibited $HER2^{-}/ER^{+}$ breast tumor growth, which indicates that PI3K/AKT/mTOR targeting could be a potential therapeutic target in breast cancer.

In the present study, we then investigated the effects of low (5 mg/kg) and high (10 mg/kg) doses of everolimus on the frequency of $CD4^{+}Foxp3^{+}$ Tregs, $CD8^{+}Foxp3^{+}$ Tregs, and CTLA-4-expressing $CD4^{+}$ and $CD8^{+}$ T cells in the bone marrow, spleen, and lymph nodes of mice-bearing breast cancer. We showed that the frequency of $CD4^{+}$ and $CD8^{+}$ T cell subsets remained unchanged in the lymphoid organs of both 10 mg/kg and 5 mg/kg treated mice compared with the vehicle group. Subsequently, our results showed that 5 mg/kg and 10 mg/kg everolimus-treated mice represented a higher frequency of $CD4^{+}Foxp3^{+}$ Tregs, $CD8^{+}Foxp3^{+}$ Tregs, as well as CTLA-4-expressing $CD4^{+}$ and $CD8^{+}$ T cells in their bone marrow, lymph nodes, and spleen compared to the vehicle-treated group. In addition, we found that everolimus treatment increased the $CD4^{+}Foxp3^{+}CTLA\text{-}4^{+}$ Treg cells frequency in the lymphoid organs of tumor-bearing mice.

In vitro stimulation of $CD4^{+}$ T cells in the presence of rapamycin significantly reduced the proliferation of $CD4^{+}$ T cells and blocked the expansion of effector $CD4^{+}CD25^{+}$ T cells, whereas it promoted $CD4^{+}CD25^{+}Foxp3^{+}$ Tregs.[26] The rapamycin-expanded cells effectively inhibited the effector functions and proliferation of $CD4^{+}$ and $CD8^{+}$ T lymphocytes.[27] Additionally, it has been shown that treatment with everolimus could promote the expansion of highly suppressive $Foxp3^{+}$ Tregs two months after therapy in metastatic renal cell carcinoma (mRCC) patients.[12,33] Our results also displayed that everolimus induced the development of Helios-expressing Tregs in the bone marrow of breast cancer-bearing mice. Helios was identified as a marker to discriminate natural or thymic-derived Tregs (Tregs) from peripheral-induced Tregs (pTregs).[28] The expression of Helios is revealed to be a marker for T cell activation and proliferation, and its expression is critical for the stable inhibitory activity of Treg cells.[29,30] In a previous study, it was shown that most $Foxp3^{+}$ Tregs co-expressed Helios, and $Foxp3^{+}Helios^{+}$Tregs had more excellent immunosuppressive properties than the $Foxp3^{+}$ $Helios^{-}$ Treg cell population.[31,32] Additionally, Treg cells cultured in the presence of rapamycin and everolimus displayed significantly higher levels of Helios and CTLA-4 expression compared to the Tregs cultured in the control group.[33] Interestingly, increased the expression of Helios by Treg cells was found to be associated with enhanced bone marrow angiogenesis in cancer-bearing mice through the vascular endothelial growth factor (VEGF)A/VEGF receptor 2 (VEGFR2) pathway.[34] However, in addition to Treg cells, Helios expression was up-regulated during Th2, and follicular helper T (Tfh) cells responded, but not Th1 in mice.[35] In our study, it is conceivable that everolimus administration might be associated with the upregulation of Helios on T cell subsets and probable recruitment to bone marrow. Therefore, Helios may be served as a novel and promising therapeutic option to manipulate Treg activity with clinical implications.

The data presented here indicate that everolimus therapy is associated with the increased frequency of $CTLA4^{+}Foxp3^{+}$ Tregs and/or $Helios^{+}Foxp3^{+}$ Tregs in the lymphoid organs of mice-bearing breast cancer. The results demonstrate that treatment with everolimus not only inhibits tumor growth but also exerts a robust immunomodulatory effect by inducing Treg cells in the lymphoid organs of breast cancer-bearing mice. These features provide a generalized suppressed state of the immune system, which may impact the differentiation and function of the various types of immune cells and ultimately drive the balance toward immunosuppression. The combination of therapy with other anti-cancer agents may negate immune suppression and enhance the therapeutic efficacy of mTOR-targeted breast cancer therapy.

CONFLICT OF INTEREST

The authors declare that there are no conflicts of interest.

ACKNOWLEDGEMENTS

The present study was part of a Ph.D. thesis written by Davoud Rostamzadeh and supported by grant no. 96/51 from the Drug Applied Research Center, Tabriz University of Medical Sciences, Tabriz, Iran. This study was financially supported by grants from Shiraz University of Medical Sciences (grant no. 95-01-16-12936 and 1396-01-01-16551(15628)) and Shiraz Institute for Cancer Research, Shiraz University of Medical Sciences (Shiraz, Iran; grant no. ICR-100-503).

REFERENCES

1. Saxton RA, Sabatini DM. mTOR Signaling in Growth, Metabolism, and Disease. Cell. 2017;168(6):960-76.
2. Dancey J. mTOR signaling and drug development in cancer. Nat Rev Clin Oncol. 2010;7(4):209-19.
3. Yang J, Nie J, Ma X, Wei Y, Peng Y, Wei X. Targeting PI3K in cancer: mechanisms and advances in clinical trials. Mol Cancer. 2019;18(1):1-28.
4. Kim LC, Cook RS, Chen J. mTORC1 and mTORC2 in cancer and the tumor microenvironment. Oncogene. 2017;36(16):2191-201.
5. Bollard J, Couderc C, Blanc M, Poncet G, Lepinasse F, Hervieu V, et al. Antitumor effect of everolimus in preclinical models of high-grade gastroenteropancreatic neuroendocrine carcinomas. Neuroendocrinology. 2013;97(4):331-40.
6. Du L, Li X, Zhen L, Chen W, Mu L, Zhang Y, et al. Everolimus inhibits breast cancer cell growth through PI3K/AKT/mTOR signaling pathway. Mol Med Rep. 2018;17(5):7163-9.
7. Boulay A, Zumstein-Mecker S, Stephan C, Beuvink I, Zilbermann F, Haller R, et al. Antitumor efficacy of intermittent treatment schedules with the rapamycin derivative RAD001 correlates with prolonged inactivation of ribosomal protein S6 kinase 1 in peripheral blood mononuclear cells. Cancer Res. 2004;64(1):252-61.
8. Yoshida-Ichikawa Y, Tanabe M, Tokuda E, Shimizu H, Horimoto Y, Miura K, et al. Overcoming the adverse effects of everolimus to achieve maximum efficacy in the treatment of inoperable breast cancer: a review of 11 cases at our hospital. Case Rep Oncol. 2018;11(2):511-20.
9. Powell JD, Pollizzi KN, Heikamp EB, Horton MR. Regulation of immune responses by mTOR. Annu Rev Immunol. 2012;30(3):39-68.
10. Nazari N, Jafari F, Ghalamfarsa G, Hadinia A, Atapour A, Ahmadi M, et al. The emerging role of microRNA in regulating the mTOR signaling pathway in immune and inflammatory responses. Immunol Cell Biol. 2021;1(2):19-21.
11. Delgoffe GM, Pollizzi KN, Waickman AT, Heikamp E, Meyers DJ, Horton MR, et al. The kinase mTOR regulates the differentiation of helper T cells through the selective activation of signaling by mTORC1 and mTORC2. Nat Immunol. 2011;12(4):295-303.
12. Rostamzadeh D, Yousefi M, Haghshenas MR, Ahmadi M, Dolati S, Babaloo Z. mTOR Signaling pathway as a master regulator of memory CD8(+) T-cells, Th17, and NK cells development and their functional properties. J Cell Physiol. 2019.
13. Delgoffe GM, Kole TP, Zheng Y, Zarek PE, Matthews KL, Xiao B, et al. The mTOR kinase differentially regulates effector and regulatory T cell lineage commitment. Immunity. 2009;30(6):832-44.
14. Battaglia M, Stabilini A, Roncarolo MG. Rapamycin selectively expands CD4+CD25+FoxP3+ regulatory T cells. Blood. 2005;105(12):4743-8.
15. Noris M, Casiraghi F, Todeschini M, Cravedi P, Cugini D, Monteferrante G, et al. Regulatory T cells and T cell depletion: role of immunosuppressive drugs. J Am Soc Nephrol. 2007;18(3):1007-18.
16. Kruisbeek AM. Isolation of mouse mononuclear cells. Curr Protoc Immunol. 2001;Chapter 3:Unit 3 1.
17. Rostamzadeh D, Haghshenas MR, Daryanoosh F, Samadi M, Hosseini A, Ghaderi A, et al. Altered frequency of CD8(+) CD11c(+) T cells and expression of immunosuppressive molecules in lymphoid organs of mouse model of colorectal cancer. J Cell Physiol. 2019;234(7):11986-98.
18. Swamydas M, Lionakis MS. Isolation, purification and labeling of mouse bone marrow neutrophils for functional studies and adoptive transfer experiments. J Vis Exp. 2013(77):e50586.
19. Zhu Y, Zhang X, Liu Y, Zhang S, Liu J, Ma Y, et al. Antitumor effect of the mTOR inhibitor everolimus in combination with trastuzumab on human breast cancer stem cells in vitro and in vivo. Tumor Biol. 2012;33(5):1349-62.
20. Browne AJ, Kubasch ML, Göbel A, Hadji P, Chen D, Rauner M, et al. Concurrent antitumor and bone-protective effects of everolimus in osteotropic breast cancer. Breast Cancer Res. 2017;19(1):1-15.
21. Ariaans G, Jalving M, De Vries EGE, De Jong S. Anti-tumor effects of everolimus and metformin are

complementary and glucose-dependent in breast cancer cells. BMC cancer. 2017;17(1):232.
22. Gorshtein A, Rubinfeld H, Kendler E, Theodoropoulou M, Cerovac V, Stalla GK, et al. Mammalian target of rapamycin inhibitors rapamycin and RAD001 (everolimus) induce anti-proliferative effects in GH-secreting pituitary tumor cells in vitro. Endocrine-related cancer. 2009;16(3):1017-27.
23. Guo H, Zhong Y, Jackson AL, Clark LH, Kilgore J, Zhang L, et al. Everolimus exhibits anti-tumorigenic activity in obesity-induced ovarian cancer. Oncotarget. 2016;7(15):20338.
24. Owonikoko TK, Zhang G, Lallani SB, Chen Z, Martinson DE, Khuri FR, et al. Evaluation of preclinical efficacy of everolimus and pasireotide in thyroid cancer cell lines and xenograft models. PLoS One. 2019;14(2):e0206309.
25. Lui A, New J, Ogony J, Thomas S, Lewis-Wambi J. Everolimus downregulates estrogen receptor and induces autophagy in aromatase inhibitor-resistant breast cancer cells. BMC cancer. 2016;16(1):1-15.
26. Battaglia M, Stabilini A, Migliavacca B, Horejs-Hoeck J, Kaupper T, Roncarolo MG. Rapamycin promotes expansion of functional CD4+CD25+FOXP3+ regulatory T cells of both healthy subjects and type 1 diabetic patients. J Immunol. 2006;177(12):8338-47.
27. Strauss L, Whiteside TL, Knights A, Bergmann C, Knuth A, Zippelius A. Selective survival of naturally occurring human CD4+CD25+Foxp3+ regulatory T cells cultured with rapamycin. J Immunol. 2007;178(1):320-9.
28. Sugimoto N, Oida T, Hirota K, Nakamura K, Nomura T, Uchiyama T, et al. Foxp3-dependent and -independent molecules specific for CD25+CD4+ natural regulatory T cells revealed by DNA microarray analysis. Int Immunol. 2006;18(8):1197-209.
29. Akimova T, Beier UH, Wang L, Levine MH, Hancock WW. Helios expression is a marker of T cell activation and proliferation. PloS one. 2011;6(8):e24226.
30. Kim H-J, Barnitz RA, Kreslavsky T, Brown FD, Moffett H, Lemieux ME, et al. Stable inhibitory activity of regulatory T cells requires the transcription factor Helios. Science. 2015;350(6258):334-9.
31. Thornton AM, Korty PE, Tran DQ, Wohlfert EA, Murray PE, Belkaid Y, et al. Expression of Helios, an Ikaros transcription factor family member, differentiates thymic-derived from peripherally induced Foxp3+ T regulatory cells. J Immunol. 2010;184(7):3433-41.
32. Zabransky DJ, Nirschl CJ, Durham NM, Park BV, Ceccato CM, Bruno TC, et al. Phenotypic and functional properties of Helios+ regulatory T cells. PloS one. 2012;7(3):e34547.
33. Huijts CM, Santegoets SJ, Quiles Del Rey M, de Haas RR, Verheul HM, de Gruijl TD, et al. Differential effects of inhibitors of the PI3K/mTOR pathway on the expansion and functionality of regulatory T cells. Clin Immunol. 2016;168:47-54.
34. Li X, Li D, Shi Q, Huang X, Ju X. Umbilical cord bloodderived Heliospositive regulatory T cells promote angiogenesis in acute lymphoblastic leukemia in mice via CCL22 and the VEGFAVEGFR2 pathway. Mol Med Rep. 2019;19(5):4195-204.
35. Serre K, Benezech C, Desanti G, Bobat S, Toellner KM, Bird R, et al. Helios is associated with CD4 T cells differentiating to T helper 2 and follicular helper T cells in vivo independently of Foxp3 expression. PLoS One. 2011;6(6):e20731.